Supplementary Information

Comprehensive Vibrational Dynamics of Half-Open Fluid-Filled Shells

Markus Lendermann[1], Jin Ming Koh[1], Joel Shi Quan Tan[2], and Kang Hao Cheong[1,3,*]

[1]Science and Math Cluster, Singapore University of Technology and Design (SUTD), 8 Somapah Road, S487372, Singapore
[2]Yong Loo Lin School of Medicine, National University of Singapore, S119228, Singapore
[3]SUTD-MIT International Design Center, Singapore University of Technology and Design
[*]Corresponding Author: kanghao_cheong@sutd.edu.sg (K. H. Cheong)

Appendix A: Undamped Numerical Model

The boundary conditions at the shell rim ($z = H$) are those of a free edge with a forcing term:

$$M_1 = 0, \qquad N_{12} - M_{12}/R_1 = 0, \tag{1a}$$
$$Q_1 + (M_{12}/B)_\theta = 0, \qquad N_1 = \cos n\theta \cos \omega t, \tag{1b}$$

where the transverse shear force Q_1 is solved from the moment equilibrium equation

$$(AM_{21})_\theta + (BM_1)_z - M_2 B_z + M_{12} A_\theta - Q_1 AB = 0, \tag{2}$$

and M_{12} and M_{21} are twisting moment components in the z and θ directions respectively. The boundary conditions for the fixed bottom of the shell ($z = z_{\text{min}}$) are

$$u = v = w = 0, \quad \theta_1 = u/R_1 + w_z/A = 0, \tag{3}$$

where θ_1 is the angle of rotation of the normal to the middle surface about tangents to the θ coordinate line. For the fluid flow modelled by the Helmholtz equation, the boundary conditions at the glass wall and free surface are

$$\nabla\phi \cdot \mathbf{e}_3|_{r=R(z)} = w_t, \tag{4a}$$
$$\phi_z + \left.\frac{\phi_{tt}}{g}\right|_{z=h} = 0, \tag{4b}$$

respectively, where g is the gravitational acceleration.

The finite difference method adopted is more conveniently implemented with a rectangular grid. To achieve a rectangular two-dimensional grid of sampling points within the fluid domain, a normalization of the radial coordinate $\eta = r/R(z)$ was performed. $N_\eta \times N_{z,\text{f}}$ points were uniformly sampled within the two-dimensional grid given by $\eta \in [0, 1]$ and $z \in [z_{\text{min}}, h]$. For the shell domain, a total of $N_{z,\text{g}}$ points were sampled within $z \in [z_{\text{min}}, H]$, of which $N_{z,\text{f}}$ were uniformly sampled within $z \in [z_{\text{min}}, h]$ while the remainder were uniformly sampled within $z \in [h, H]$. $N_{z,\text{f}}$ and $N_{z,\text{g}}$ were determined by the initial desired number of sampling points along the z direction N_z as follows:

$$N_{z,\text{f}} = \max\left(\lceil N_z/10\rceil, \lfloor hN_z/H\rfloor\right), \tag{5a}$$
$$N_{z,\text{g}} = N_{z,\text{f}} + \max\left(\lceil N_z/10\rceil, N_z - N_{z,\text{f}}\right), \tag{5b}$$

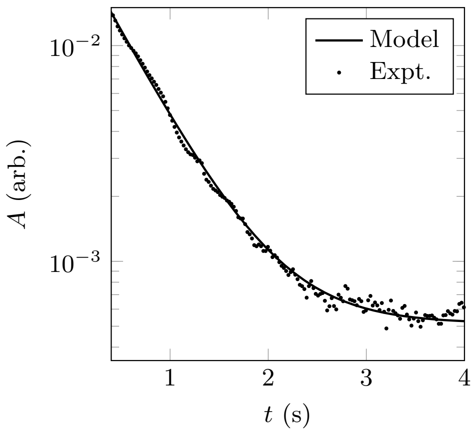

Figure 1: Measured and best-fit amplitude decay profiles of an empty wineglass, from which time constant $\tau = 0.515\,\mathrm{s}$ and $\sigma = 3.50 \times 10^{-4}$ were obtained.

ensuring sufficient grid points in the fluid and shell domains for low and high fluid levels respectively.

In the extension of the model with a solid object inserted into the fluid domain, the radial coordinate is normalized as $\eta = [r - R_\mathrm{i}(z)]/[R(z) - R_\mathrm{i}(z)] \in [0, 1]$ such that a rectangular grid is maintained. An additional boundary condition $\nabla\phi \cdot \mathbf{n}_\mathrm{o}|_{r=R_\mathrm{i}(z)} = 0$, where $\mathbf{n}_\mathrm{o}$ is the normal vector to the surface of the solid object, is introduced.

Appendix B: Damped Numerical Model

For the fluid flow modelled by the linearized Navier-Stokes equations, the boundary conditions at the shell wall and the free surface are

$$\mathbf{u}' = u_t\mathbf{e}_1 + v_t\mathbf{e}_2 - w_t\mathbf{e}_3 \qquad \text{at } r = R(z), \tag{6a}$$

$$\mathbf{u}' = \mathbf{0} \qquad \text{at } z = 0, \tag{6b}$$

$$\frac{\partial p}{\partial t} = 2\mu\frac{\partial^2 u_z'}{\partial z \partial t} + \rho_\mathrm{f} g u_z' \qquad \text{at } z = H, \tag{6c}$$

$$\frac{\partial u_z'}{\partial r} + \frac{\partial u_r'}{\partial z} = 0, \; \frac{\partial u_\theta'}{\partial z} + \frac{1}{r}\frac{\partial u_z'}{\partial \theta} = 0 \qquad \text{at } z = H. \tag{6d}$$

Appendix C: Glass Characterization

The shape $R(z)$ and thickness $d(z)$ profiles of each wineglass were characterized as follows. For the outer surface profile, a photograph of the wineglass filled with dyed water placed in front of a backlit screen was taken. Computational edge detection then yielded the outer profile. The thickness profile was obtained by detecting the vertical change in fluid level δz with a travelling microscope when a small known volume of dyed ethanol δV was added. Where these measurements were taken, the outer radius R_o was measured with a vernier caliper. Thus, the wineglass thickness is given by $R_\mathrm{o} - \sqrt{\delta V/\pi\delta z}$. The neutral surface is then taken to be equidistant from the measured outer and inner profiles. To facilitate computation in our models, the measured shape and thickness profiles are converted into closed-form expressions by fitting them to polynomials given by $R(z) = \sum_{i=1}^{9} a_i z^{i/4}$ and $d(z) = \sum_{i=1}^{16} b_i z^{i/4}$, where a_i and b_i are coefficients determined by the least-squares method.

The complex Young's modulus $Y' = Y(1 + \sigma j)$ of the glass material in the numerical damped model was also characterized. The real part $\mathrm{Re}\{Y'\} = Y$ was determined via nonlinear regression of model calculations of empty-glass natural frequency ω_d against measured values. The imaginary part $\mathrm{Im}\{Y'\} = Y\sigma$ was characterized via nonlinear regression of computed decay time constants against experimental values, measured by exciting the wineglass to steady-state through the horn driver, and then recording the amplitude decay profile upon abrupt deactivation of the driver. Decay profiles are assumed to be of the form $A(t) = \exp\left(-(t - a_1)/\tau\right) + a_2$, where τ is the time constant and a_i are constants to be determined. σ is then obtained by choosing an appropriate value such that the theoretical quality factor Q of the empty wineglass is related to τ and the natural frequency ω_d by $2Q = \tau\omega_d$. Figure 1 presents a sample measured decay profile and best-fit computed profile as obtained from the procedure. Characterized Y and σ values are given in Table 1 of the main paper.